

Riemann problem for constant flow with single-point heating source

Changsheng Yu, Chengliang Feng, Zhiqiang Zeng, Tiegang Liu

March 8, 2022

Abstract

This work focuses on the Riemann problem of Euler equations with global constant initial conditions and a single-point heating source, which comes from the physical problem of heating one-dimensional inviscid compressible constant flow. In order to deal with the source of Dirac delta-function, we propose an analytical frame of double classic Riemann problems(CRPs) coupling, which treats the fluids on both sides of the heating point as two separate Riemann problems and then couples them. Under the double CRPs frame, the solution is self-similar, and only three types of solution are found. The theoretical analysis is also supported by the numerical simulation. Furthermore, the uniqueness of the Riemann solution is established with some restrictions on the Mach number of the initial condition.

Keywords: hyperbolic balance law, non-homogeneous Euler equations, δ -singularity, Riemann problem

AMS subject classifications: 35L81,80A20

1 Introduction

The Riemann problem of the one-dimensional inviscid compressible flow with global constant initial conditions and a single-point heating source is studied in this paper. The heating point is located at $x = 0$. The governing equations is given by

$$\frac{\partial U}{\partial t} + \frac{\partial F}{\partial x} = S, \quad (1.1)$$

where

$$U = \begin{pmatrix} \rho \\ \rho u \\ E \end{pmatrix}, F = \begin{pmatrix} \rho u \\ \rho u^2 + p \\ (E + p)u \end{pmatrix}, S = \begin{pmatrix} 0 \\ 0 \\ Q\delta(x) \end{pmatrix}.$$

Here, ρ , p and E denote the thermodynamical variables: density, pressure and total energy, respectively. u is velocity. $Q > 0$ is the heat flux per unit time added to the flow. $\delta(x)$ is the Dirac delta-function. The source means that Q heat is added to the flow from the heating point per unit time in the physical sense. We assume that the fluid is polytropic ideal and the equation of state is given by

$$p = (\gamma - 1)\rho e, \quad 1 \leq \gamma \leq 3.$$

where γ is the ratio of specific heats and e is the internal energy. The initial condition is

$$U(x, 0) \equiv U_1 = (\rho_1, \rho_1 u_1, E_1), \quad (1.2)$$

where ρ_1 , u_1 and E_1 are constant. There is no loss of generality in assuming $u_1 > 0$. The subscript "1" means the initial state in this paper. The physical problem described by the Riemann problem (1.1) and (1.2) is that Q heat is added to the one-dimensional constant flow per unit time, as shown in Figure 1.

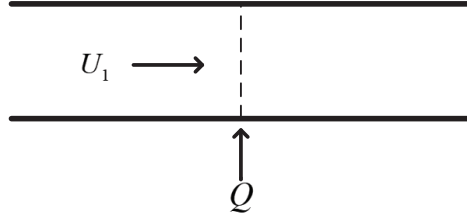


Figure 1: one-dimensional constant flow with heat addition from a single point

The subscripts "-" and "+" denote the limiting states upstream and downstream of the heating point, respectively. Write

$$U_-(t) = U(0-, t), \quad U_+(t) = U(0+, t).$$

The source term implies a jump of the energy flux across the heating point.

$$\rho_-(t)u_-(t) = \rho_+(t)u_+(t) \quad (1.3a)$$

$$\rho_-(t)u_-(t)^2 + p_-(t) = \rho_+(t)u_+(t)^2 + p_+(t) \quad (1.3b)$$

$$(E_-(t) + p_-(t))u_-(t) + Q = (E_+(t) + p_+(t))u_+(t). \quad (1.3c)$$

If the velocity at the heating point is zero, thermal convection does not take effect, then the heat addition has no effect on the flow. Thus in the remainder of this paper we assume that

$$u_-(t) \neq 0, \quad u_+(t) \neq 0.$$

We only deal with the situation of constant $U_-(t)$ and $U_+(t)$. Omitting the time parameter t , we can get the following equation from (1.3).

$$\left(\frac{1}{2}u_-^2 + h_-\right)(1+k) = \frac{1}{2}u_+^2 + h_+,$$

where h is enthalpy. $k = \frac{Q}{\rho_-(t)u_-(t)\left(\frac{1}{2}u_-^2 + h_-\right)}$ is called the heating parameter and is assumed to be a constant parameter.

The heating equations are defined by

$$\begin{cases} \rho_- u_- = \rho_+ u_+ \\ \rho_- u_-^2 + p_- = \rho_+ u_+^2 + p_+ \\ \left(\frac{1}{2}u_-^2 + h_-\right)(1+k) = \frac{1}{2}u_+^2 + h_+ \end{cases}. \quad (1.4)$$

The solution of the heating equations (1.4) corresponds to a steady solution of the equations (1.1).

The mathematical model of Figure 1 can be applied to the study of one-dimensional condensation problem (see [8, 9]). The condensation of the vapor leads to the release of latent heat and therefore has heating effects on the carrier fluid. Previous researches on condensation problems have revealed some information about the solution of Riemann problem (1.1) and (1.2). The solution of the heating equations (1.4) has already been available in [7–9, 20]. In [20] Schnerr made a good summary of the properties of the solution to (1.4) at the case of $M_- > 1$, which is typical for condensation problems. Schnerr showed that there are two solutions of the heating equations (1.4), one called the shock solution, which reduces to identity when $Q = 0$, and the other called the weak solution, which reduces to the adiabatic normal shock solution when $Q = 0$. For the heat addition of subsonic flow, Schnerr predicted the appearance of the unsteady solution, but did not do a more detailed analysis. For the unsteady solution of this Riemann problem, Dongen et al. [9] studied the unsteady effects of the heat addition, and proposed three possible solution structures. Those three structures are determined by the Mach numbers of the fluid around the heating point. However, a complete and rigorous theoretical proof is lacking at present. On the other hand, numerical simulation as an effective tool has

been employed to explore the wave patterns of the heating problem. Chengwan et al. [6] used the ASCE method [17] to numerically verify the above three structures by the simulation of the onset of condensation in a slender Laval nozzle. In the wet nitrogen condensation problem of the Laval nozzle, Chengwan showed the transition between the three structures by adjusting the humidity. To our knowledge, there is no effective theoretical method to study the exact solution of Riemann problem (1.1) and (1.2).

Conservative hyperbolic equations with source terms can be transformed into non-conservative hyperbolic equations without source terms. Adopting the following form for the δ -function

$$\delta(x) = \frac{\partial H(x)}{\partial x}, \quad H(x) = \begin{cases} 0, & x < 0 \\ 1, & x > 0 \end{cases},$$

where $H(x)$ is called Heaviside function, one can rewrite the Riemann problem (1.1) and (1.2) into following non-conservative form.

$$\frac{\partial \tilde{U}}{\partial t} + \tilde{A} \frac{\partial \tilde{U}}{\partial x} = 0, \quad (1.5)$$

where

$$\tilde{U} = \begin{pmatrix} \rho \\ \rho u \\ E \\ h \end{pmatrix}, \quad \tilde{A} = \begin{pmatrix} 0 & 1 & 0 & 0 \\ \frac{1}{2}(\gamma - 3)u^2 & (3 - \gamma)u & \gamma - 1 & 0 \\ \frac{1}{2}(\gamma - 2)u^3 - \frac{c^2 u}{\gamma - 1} & \frac{3 - 2\gamma}{2}u^2 + \frac{c^2}{\gamma - 1} & \gamma u & -Q \\ 0 & 0 & 0 & 0 \end{pmatrix},$$

where c is the speed of sound. The initial condition for the augmented equations is

$$\tilde{U}(x, 0) = \left(\rho_0 \quad \rho_0 u_0 \quad E_0 \quad H(x) \right)^T.$$

By defining proper entropy solution for non-conservative equations (1.5), one can analyzed the solutions of the original Riemann problem and design appropriate numerical methods to make numerical simulation (see [1, 10, 11]). Applications of that method include the fluid in a nozzle with discontinuous cross-sectional area(see [13, 14, 21]) and the shallow water equations with discontinuous topography(see [2, 5, 15, 18, 22]). The augmented equations (1.5) give rise to an additional linearly degenerated characteristic field and an additional stationary discontinuity. Although the augmented equations do not contain source terms, the solution process of the Riemann problem is very complex and often problem-related due to the lack of conservation or strict hyperbolicity.

The Riemann problem of homogeneous Euler equations with piecewise constant initial conditions is called classical Riemann problem(CRP). Although the addition of the source term

does not lead to the loss of self-similarity, the singularity of the source term has a significant effect on the structure of the solution. The Riemann solution of the Euler equations with smooth source terms, which are often called generalized Riemann problem (GRP, see [3, 4, 24, 25]), has the same wave patterns as the Riemann solution of its corresponding homogeneous Euler equations. However, the singularity source term affects the wave patterns of the Riemann solution. In fact, as can be seen from [8], the solution of Riemann problem (1.1) and (1.2) may be a four waves structure or a five waves structure, which is far different from the wave structure of the CRP.

In this work, an analytical frame, which is called the double CRPs frame, is proposed to construct the exact solution of the Riemann problem (1.1) and (1.2). It regards the fluids on both sides of the heating point as two separate CRPs, and gives the upper limit of the number of waves first. The solutions of the two CRPs are then coupled on the premise of maintaining the physical properties of the heating point. Depending on the heating properties and gasdynamics properties, the extra waves are deleted and the type of wave is finally determined. One advantage of the double CRPs frame is that it is independent of whether the fluid at the heating point is supersonic or subsonic. Under this frame we demonstrate three possible structures of the solution, which are verified by numerical tests in Section 5.

The text is arranged as follows. In Section 2, we will introduce the solution of the heating equations and derive several useful properties. In Section 3, an analytical frame of double CRPs coupling will be introduced to constructively solve the Riemann problem (1.1) and (1.2). Under this frame We will prove that there are at most three types of the solution. In Section 4, the structure of the solution will be associated with the Mach number of the incoming flow to illustrate the uniqueness of the solution. In Section 5, we will give an iterative method for the solution of each structure. Then we will give five tests for the Riemann problem (1.1) and (1.2) with different initial conditions and heating coefficients. Finally, a brief summary will be given in Section 6.

2 Solutions of the heating equations

According to [20], there are two branches of the solution to the heating equations (1.4). We can choose the physical solution from these two branches by the following property.

Property 2.1 *If $M_- < 1$, then $M_+ \leq 1$. If $M_- > 1$, then $M_+ \geq 1$.*

The physical solution corresponds to the weak solution in [20]. In this paper the expression

of Dongen et al. [9] is adopted. For the heat addition of subsonic flow, the solution is

$$I \equiv \sqrt{\left(\gamma + \frac{1}{M_-^2}\right)^2 - 2(\gamma + 1)\left(\frac{1}{M_-^2} + \frac{\gamma - 1}{2}\right)(1 + \kappa)}, \quad (2.1a)$$

$$\frac{u_+}{u_-} = \frac{\rho_-}{\rho_+} = \frac{1}{\gamma + 1} \left(\gamma + \frac{1}{M_-^2} - I\right), \quad (2.1b)$$

$$\frac{p_+}{p_-} = \frac{M_-^2}{\gamma + 1} \left(\gamma + \frac{1}{M_-^2} + \gamma I\right), \quad (2.1c)$$

$$M_+ = \sqrt{\frac{\gamma + \frac{1}{M_-^2} - I}{\gamma + \frac{1}{M_-^2} + \gamma I}}. \quad (2.1d)$$

For the heat addition of supersonic flow, the solution is

$$I \equiv \sqrt{\left(\gamma + \frac{1}{M_-^2}\right)^2 - 2(\gamma + 1)\left(\frac{1}{M_-^2} + \frac{\gamma - 1}{2}\right)(1 + \kappa)}, \quad (2.2a)$$

$$\frac{u_+}{u_-} = \frac{\rho_-}{\rho_+} = \frac{1}{\gamma + 1} \left(\gamma + \frac{1}{M_-^2} + I\right), \quad (2.2b)$$

$$\frac{p_+}{p_-} = \frac{M_-^2}{\gamma + 1} \left(\gamma + \frac{1}{M_-^2} - \gamma I\right), \quad (2.2c)$$

$$M_+ = \sqrt{\frac{\gamma + \frac{1}{M_-^2} + I}{\gamma + \frac{1}{M_-^2} - \gamma I}}. \quad (2.2d)$$

M is Mach number. The advantage of this expression is that the ratios of variables before and after heat addition are only related to the upstream Mach number of the heating point. In order to make the solution reasonable, there is an upper bound on k as follows.

$$k \leq k_{max} \stackrel{def}{=} \frac{(1 - M_-^2)^2}{2(\gamma + 1)M_-^2 \left(1 + \frac{\gamma - 1}{2}M_-^2\right)}. \quad (2.3)$$

k_{max} is called maximum heating parameter. The relation between k_{max} and M_- is shown in Figure 2. When $M_- \rightarrow 0+$, k_{max} approaches asymptotically $+\infty$. When $M_- \rightarrow \infty$, k_{max} approaches asymptotically a finite number $\frac{1}{\gamma^2 - 1}$. The roots of the equation

$$k = \frac{(1 - M^2)^2}{2(\gamma + 1)M^2 \left(1 + \frac{\gamma - 1}{2}M^2\right)} \quad (2.4)$$

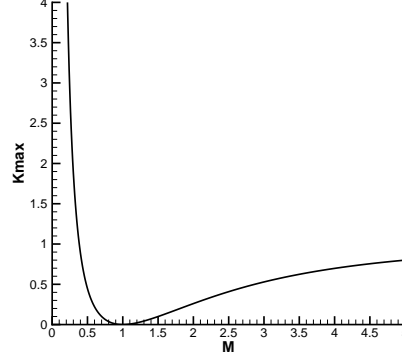


Figure 2: Relation between the maximum heating parameter and the upstream Mach number of the heating point.

are

$$M^{1,2} = \begin{cases} \sqrt{\frac{k(\gamma+1)+1 \pm (\gamma+1)\sqrt{k(k+1)}}{1-k(\gamma^2-1)}}, & \text{if } k(\gamma^2 - 1) \neq 1 \\ \sqrt{\frac{1}{2[k(\gamma+1)+1]}}, & \text{if } k(\gamma^2 - 1) = 1 \end{cases}$$

We denote

$$M_* = \begin{cases} \sqrt{\frac{k(\gamma+1)+1 - (\gamma+1)\sqrt{k(k+1)}}{1-k(\gamma^2-1)}}, & \text{if } k(\gamma^2 - 1) \neq 1 \\ \sqrt{\frac{1}{2[k(\gamma+1)+1]}}, & \text{if } k(\gamma^2 - 1) = 1 \end{cases}$$

$$M_{**} = \begin{cases} \sqrt{\frac{k(\gamma+1)+1 + (\gamma+1)\sqrt{k(k+1)}}{1-k(\gamma^2-1)}}, & \text{if } k(\gamma^2 - 1) < 1 \\ +\infty, & \text{if } k(\gamma^2 - 1) \geq 1 \end{cases}$$

It can easily be checked that $0 < M_* < 1$ and $M_{**} > 1$, thus we arrive at the following conclusion.

Lemma 2.1

- (i) If $k(\gamma^2 - 1) < 1$, then $M_- \leq M_*$ or $M_- \geq M_{**}$.
- (ii) If $k(\gamma^2 - 1) \geq 1$, then $M_- \leq M_*$.
- (iii) If $M_- = M_*$ or $M_- = M_{**}$, then $I = 0$ and $M_+ = 1$.

Lemma 2.2 *If $k(\gamma^2 - 1) < 1$, we have*

$$M_* = \sqrt{\frac{(\gamma - 1)M_{**}^2 + 2}{2\gamma M_{**}^2 - \gamma + 1}}, \quad M_{**} = \sqrt{\frac{(\gamma - 1)M_*^2 + 2}{2\gamma M_*^2 - \gamma + 1}}. \quad (2.5)$$

The proof is trivial.

The downstream fluid is called thermal choked if $M_+ = 1$. If the upstream fluid is sonic, then $k_{max} = 0$, which means that any heat addition is not allowed for the sonic flow. We now turn to the relations of the upstream and downstream fluids.

Theorem 2.1 *For the heat addition of subsonic flow we have $u_+ > u_-$, $p_+ < p_-$, $\rho_+ < \rho_-$ and $M_+ > M_-$. For the heat addition of supersonic flow we have $u_+ < u_-$, $p_+ > p_-$, $\rho_+ > \rho_-$ and $M_+ < M_-$.*

Proof 2.1 *For the heat addition of subsonic fluid, $k > 0$ implies*

$$\begin{aligned} I &< \sqrt{\left(\gamma + \frac{1}{M_-^2}\right)^2 - 2(\gamma + 1)\left(\frac{1}{M_-^2} + \frac{\gamma - 1}{2}\right)} = \frac{1}{M_-^2} - 1, \\ \frac{u_+}{u_-} &> \frac{1}{\gamma + 1} \left(\gamma + \frac{1}{M_-^2} + 1 - \frac{1}{M_-^2}\right) = 1, \\ \frac{\rho_+}{\rho_-} &= \frac{u_-}{u_+} < 1, \\ \frac{p_+}{p_-} &< \frac{M_-^2}{\gamma + 1} \left(\gamma + \frac{1}{M_-^2} - \gamma + \frac{\gamma}{M_-^2}\right) = 1, \\ M_+ &= \sqrt{\frac{\gamma + \frac{1}{M_-^2} - I}{\gamma + \frac{1}{M_-^2} + \gamma I}} > \sqrt{\frac{\gamma + \frac{1}{M_-^2} - \frac{1}{M_-^2} + 1}{\gamma + \frac{1}{M_-^2} + \gamma\left(\frac{1}{M_-^2} - 1\right)}} = M_-. \end{aligned}$$

For the heat addition of supersonic fluid, $k > 0$ implies

$$\begin{aligned} I &< \sqrt{\left(\gamma + \frac{1}{M_-^2}\right)^2 - 2(\gamma + 1)\left(\frac{1}{M_-^2} + \frac{\gamma - 1}{2}\right)} = 1 - \frac{1}{M_-^2}, \\ \frac{u_+}{u_-} &< \frac{1}{\gamma + 1} \left(\gamma + \frac{1}{M_-^2} + 1 - \frac{1}{M_-^2}\right) = 1, \\ \frac{\rho_+}{\rho_-} &= \frac{u_-}{u_+} > 1, \\ \frac{p_+}{p_-} &> \frac{M_-^2}{\gamma + 1} \left(\gamma + \frac{1}{M_-^2} - \gamma + \frac{\gamma}{M_-^2}\right) = 1, \\ M_+ &= \sqrt{\frac{\gamma + \frac{1}{M_-^2} + I}{\gamma + \frac{1}{M_-^2} - \gamma I}} < \sqrt{\frac{\gamma + \frac{1}{M_-^2} - \frac{1}{M_-^2} + 1}{\gamma + \frac{1}{M_-^2} + \gamma\left(\frac{1}{M_-^2} - 1\right)}} = M_-. \end{aligned}$$

Given any $k > 0$ and $1 < \gamma < 3$, we define

$$\begin{aligned}\phi(M) &= \frac{1}{\gamma+1} \left(\gamma + \frac{1}{M^2} - I \right), \\ \psi(M) &= \frac{M^2}{\gamma+1} \left(\gamma + \frac{1}{M^2} + \gamma I \right),\end{aligned}$$

where

$$I = \sqrt{\left(\gamma + \frac{1}{M^2} \right)^2 - 2(\gamma+1) \left(\frac{1}{M^2} + \frac{\gamma-1}{2} \right) (1+\kappa)}.$$

According to 2.1 and 2.2, $\frac{u_+}{u_-}$ and $\frac{p_+}{p_-}$ are both functions of M_- . For the subsonic heat addition, we have

$$\frac{u_+}{u_-} = \frac{\rho_-}{\rho_+} = \phi(M_-), \quad \frac{p_+}{p_-} = \psi(M_-). \quad (2.6)$$

A tedious computation gives the following theorem.

Theorem 2.2 $\phi'(M) > 0, \quad \psi'(M) < 0.$

3 Structure of solution

A basic assumption of our double CRPs frame is that $U_-(t)$ and $U_+(t)$ are both constant vectors. The solution $U(x, t)$ of the Riemann problem (1.1) and (1.2) satisfies the homogeneous Euler equations in both the left half $\{(x, t) | x < 0, t \geq 0\}$ and the right $\{(x, t) | x > 0, t \geq 0\}$. Consequently, $U(x, t)$ is self-similar. The exact solution in this paper refers to the self-similar solution under this frame.

The exact solution $U(x, t)$ in the left half $\{(x, t) | x < 0, t \geq 0\}$ satisfies the classical Euler equations, hence is the left half of the CRP solution with U_1 and $U(0-, t)$ as the left and right initial conditions. From the theory of CRP solution, we know that $U(x, t)$ in the left half consists three discontinuities at most, which are two genuinely nonlinear waves, namely shock waves or rarefaction waves, and a contact discontinuity corresponding to the characteristic fields $u - a$, $u + a$ and u , respectively. Similarly, $U(x, t)$ in the right half consists two genuinely nonlinear waves and a contact discontinuity at most.

Theorem 3.1 *The self-similar solution of the Riemann problem (1.1) and (1.2) consists of seven discontinuities at most. They are a heating discontinuity at $x = 0$, two genuinely nonlinear waves and a contact discontinuity left to $x = 0$, two genuinely nonlinear waves and a contact discontinuity right to $x = 0$ respectively, as shown in Figure 3.*

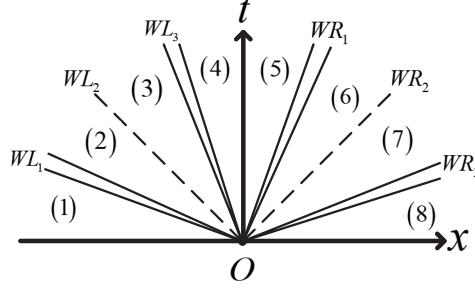


Figure 3: All possible waves for the Riemann problem (1.1) and (1.2)

The elementary waves on the left and right sides are denoted as WL_1, WL_2, WL_3 and WR_1, WR_2, WR_3 , respectively. The eight constant regions are labeled (1) ~ (8), respectively. $U_1 \sim U_8$ are the states in regions (1) ~ (8) and it is clear that $U_1 = U_8$. Note that the t -axis is a discontinuity and $U_4 \neq U_5$. We adopt similar way to express the solution structure as in [21]. For examples, $S(U_1, U_2)$ and $R(U_1, U_2)$ mean two states U_1 and U_2 are connected by a shock and a rarefaction wave respectively, $C(U_2, U_3)$ means U_2 and U_3 are connected by a contact discontinuity, and $H(U_4, U_5)$ means U_4 and U_5 are connected by a heating discontinuity. All the six elementary waves in Figure 3 can not exist at the same time. The next step in our double CRPs coupling method is to eliminate the redundant waves according to the heat addition properties and the gasdynamics properties. We will give the main results in Theorem 3.2.

Theorem 3.2 *Under the double CRPs frame, there are three different structures of the exact solution to the Riemann problem (1.1) and (1.2) as follows.*

(1) *Type 1: if $M_4 < M_5 < 1$, then the structure could be*

$$S(U_1, U_4) \oplus H(U_4, U_5) \oplus C(U_5, U_7) \oplus S(U_7, U_8)$$

(2) *Type 2: if $M_4 < M_5 = 1$, then the structure could be*

$$S(U_1, U_4) \oplus H(U_4, U_5) \oplus R(U_5, U_6) \oplus C(U_6, U_7) \oplus S(U_7, U_8)$$

(3) *Type 3: if $M_4 > M_5 \geq 1$, then the structure could be*

$$H(U_1, U_5) \oplus R(U_5, U_6) \oplus C(U_6, U_7) \oplus S(U_7, U_8)$$

Figure 3 depicts the three wave patterns in Theorem 3.2. They will be denoted by Type 1, Type 2 and Type 3, respectively. According to the Mach number at the heating point and whether the thermal choked state appears, the proof of the Theorem 3.2 falls naturally into three parts: Lemma 3.1, Lemma 3.2 and Lemma 3.3, which correspond to Type 1, Type 2 and Type 3, respectively.

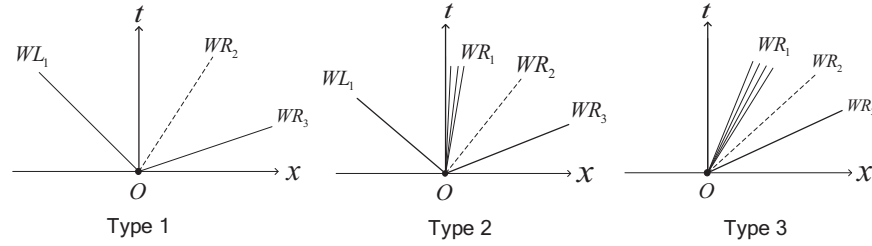


Figure 4: Three different structures of the exact solution to the Riemann problem (1.1) and (1.2).

Lemma 3.1 *Under the double CRPs frame, if $M_4 < M_5 < 1$, then WL_2 , WL_3 and WR_1 do not exist, and then $u_5 > u_4 > 0$; if WL_1 and WR_3 exist, they are both shock waves.*

Proof 3.1 *We first outline the proof. The problem is reduced to the determination of the upstream fluid U_4 and the downstream fluid U_5 (either of which can be determined by the other) at the heating point, such that U_4 and U_1 can be connected by the fundamental waves with non-positive speed, and that U_5 and $U_8 = U_1$ can be connected by the fundamental waves with non-negative speed.*

According to (1.3), it follows that u_4 and u_5 have the same sign. WL_3 and WR_1 do not exist since $M_4 < 1$ and $M_5 < 1$. There are three cases for the sign of the velocity at heating point, as follows.

- (1) *If $u_4 > 0$, then $u_5 > 0$ and WL_2 does not exist;*
- (2) *If $u_4 < 0$, then $u_5 < 0$ and WR_2 does not exist;*
- (3) *If $u_4 = u_5 = 0$, then both the speeds of WL_2 and WR_2 are zero and the widths of region 3 and region 6 are both zero.*

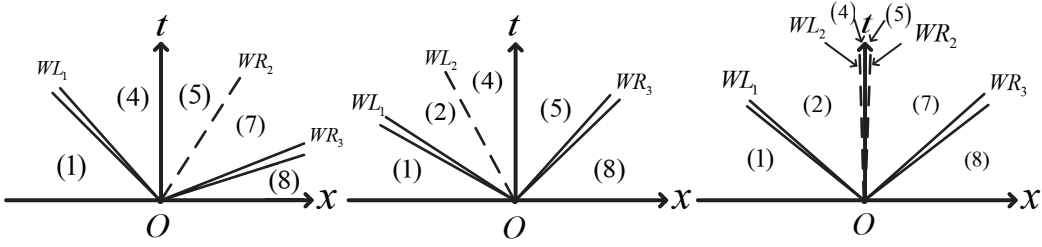


Figure 5: Three possible structures when subsonic flow is heated without thermal choke.

These three structures are shown in Figure 3.1.

If $u_4 < 0, u_5 < 0$, then WL_1 is a shock wave and WR_3 is a rarefaction wave. From Theorem 2.1 we have $p_4 < p_5$. The relations of the elementary wave (see for instance [23]) imply $p_1 \leq p_2 = p_4$ and $p_5 \leq p_8$. It results $p_5 \leq p_1$, which is contradictory with $p_5 > p_4 \geq p_1$, hence the structure of $u_4 < 0, u_5 < 0$ does not exist.

Using a similar method we can prove that the structure of $u_4 = u_5 = 0$ does not exist. The structure of the solution is the left figure in Figure 5.

The next thing to do is to prove that WL_1 is a shock. If the assertion would not hold, then WL_1 is a rarefaction wave, which implies $p_7 = p_5 < p_4 \leq p_1 = p_8$. It follows that WR_3 is a rarefaction wave and $u_7 = u_5 > u_4 \geq u_1$. Applying the conservations of mass and momentum at the control volume $[x_0, x_4] \times [0, T]$ in the $x-t$ space, as shown in the left figure of Figure 3.1, we have

$$\int_{x_0}^{x_4} \rho(x, T) dx = \int_{x_0}^{x_4} \rho(x, 0) dx,$$

$$\int_{x_0}^{x_4} \rho(x, T) u(x, T) dx = \int_{x_0}^{x_4} \rho(x, 0) u(x, 0) dx.$$

U is constant at each region, thus

$$\begin{aligned} & \int_{x_0}^{x_1} \rho(x, T) dx + \rho_4 |x_1| + \rho_5 |x_2| + \rho_7 |x_3 - x_2| + \int_{x_3}^{x_4} \rho(x, T) dx \\ &= \int_{x_0}^{x_1} \rho(x, T) \frac{u(x, T)}{u_1} dx + \rho_4 |x_1| \frac{u_4}{u_1} + \rho_5 |x_2| \frac{u_5}{u_1} + \rho_7 |x_3 - x_2| \frac{u_7}{u_1} + \int_{x_3}^{x_4} \rho(x, T) \frac{u(x, T)}{u_1} dx. \end{aligned} \quad (3.1)$$

The velocity inside the rarefaction wave is monotonous, it follows that $u(x, T) \geq \max\{u_1, u_4\} \geq u_1$ for $x_0 \leq x \leq x_1$ and $u(x, T) \geq \max\{u_5, u_8\} = u_5 > u_1$ for $x_3 \leq x \leq x_4$, which imply

$$\int_{x_0}^{x_1} \rho(x, T) \frac{u(x, T)}{u_1} dx \geq \int_{x_0}^{x_1} \rho(x, T) dx,$$

$$\int_{x_3}^{x_4} \rho(x, T) \frac{u(x, T)}{u_1} dx \geq \int_{x_3}^{x_4} \rho(x, T) dx.$$

$\frac{u_4}{u_1} \geq 1$, $\frac{u_5}{u_1} > 1$ and $\frac{u_7}{u_1} > 1$ hold for the right side of Lemma 3.1. Substituting the above inequalities to Lemma 3.1, we have $x_2 = x_3 = 0$ and $u_5 = 0$, which leads to a contradiction.

Finally, we have to show that WR_3 is a shock. If the assertion is false, then WR_3 is a non-degenerate rarefaction wave, which implies $u_4 < u_5 = u_7 \leq u_8 = u_1$. Applying the conservations of mass and momentum at the control volume $[x_0, x_3] \times [0, T]$ in the $x-t$ space, as shown in the right figure of Figure 3.1, we have

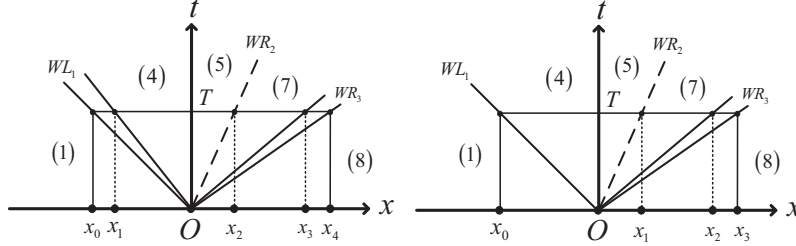


Figure 6: The integral diagram in the proof of Lemma 3.1. Left: WL_1 is a rarefaction wave and WR_3 is a rarefaction wave. Right: WL_1 is a shock and WR_3 is a rarefaction wave.

$$\int_{x_0}^{x_3} \rho(x, T) dx = \int_{x_0}^{x_3} \rho(x, 0) dx,$$

$$\int_{x_0}^{x_3} \rho(x, T) u(x, T) dx = \int_{x_0}^{x_3} \rho(x, 0) u(x, 0) dx.$$

Thus

$$\rho_4|x_0| + \rho_5|x_1| + \rho_7|x_2 - x_1| + \int_{x_2}^{x_3} \rho(x, T) dx$$

$$= \rho_4|x_0| \frac{u_4}{u_1} + \rho_5|x_1| \frac{u_5}{u_1} + \rho_7|x_2 - x_1| \frac{u_7}{u_1} + \int_{x_2}^{x_3} \rho(x, T) \frac{u(x, T)}{u_1} dx.$$

For the velocity u insides the rarefaction wave WR_3 , we have $u(x, T) \leq \max(u_5, u_8) = u_8 = u_1$, which implies

$$\int_{x_2}^{x_3} \rho(x, T) \frac{u(x, T)}{u_1} dx \leq \int_{x_2}^{x_3} \rho(x, T) dx.$$

$\frac{u_4}{u_1} < 1$, $\frac{u_5}{u_1} \leq 1$ and $\frac{u_7}{u_1} \leq 1$ hold for the right side of Lemma 3.1. We see at once that $\frac{u_7}{u_1} = 1$ and $U_7 = U_8$, which leads to a contradiction.

The following two lemmas can be proved using a similar method.

Lemma 3.2 *Under the double CRPs frame, if $M_4 < M_5 = 1$, then WL_2 and WL_3 do not exist, and then $u_5 > u_4 > 0$; if WL_1 , WR_1 and WR_3 exist, they are a shock, a rarefaction wave and a shock, respectively.*

Lemma 3.3 *Under the double CRPs frame, if $M_4 > M_5 \geq 1$, then WL_1, WL_2 and WL_3 do not exist, and then $u_5 > u_4 > 0$; if WR_1 and WR_3 exist, they are a rarefaction wave and a shock, respectively.*

Compared with Type 1 and Type 3, Type 2 has one more wave, and the condition $M_5 = 1$ is used to match the number of conditions at this time. In the remainder of this paper, each wave and each constant region are denoted as in Figure 3.

4 Uniqueness of solution

In this section, we will make a preliminary exploration of the uniqueness of the solution.

A more refined analysis of the exact solution needs to involve the quantitative relations of the fundamental waves and the heating discontinuity. We begin by defining five functions to connect the states on the left and right sides of the shock wave WL_1 , which appears in the solution of Type 1 and Type 2.

$$\begin{aligned}
 f_1(M_1, M_2) &\stackrel{def}{=} \frac{(\gamma + 1)(M_1 - M_2)^2}{(\gamma - 1)(M_1 - M_2)^2 + 2}, \\
 f_2(M_1, M_2) &\stackrel{def}{=} \frac{2\gamma(M_1 - M_2)^2 - \gamma + 1}{\gamma + 1}, \\
 f_3(M_1, M_2) &\stackrel{def}{=} \frac{(\gamma - 1)(M_1 - M_2)^2 + 2}{(\gamma + 1)(M_1 - M_2)^2}, \\
 f_4(M_1, M_2) &\stackrel{def}{=} f_3(M_1, M_2) + \frac{M_2}{M_1}(1 - f_3(M_1, M_2)), \\
 f_5(M_1, M_2) &\stackrel{def}{=} \frac{((\gamma - 1)M_1 + 2M_2)(M_1 - M_2) + 2}{[2\gamma(\gamma - 1)(M_1 - M_2)^4 + (6\gamma - \gamma^2 - 1)(M_1 - M_2)^2 - 2(\gamma - 1)]^{\frac{1}{2}}}.
 \end{aligned}$$

Applying the Rankine-Hugoniot conditions

$$F(U_4) - F(U_1) = s_L(U_4 - U_1),$$

where s_L is the speed of WL_1 , we deduce that

$$\begin{aligned}
 \rho_4/\rho_1 &= f_1(M_1, M_{SL}), & p_4/p_1 &= f_2(M_1, M_{SL}), \\
 (u_4 - s_L)/(u_1 - s_L) &= f_3(M_1, M_{SL}), & u_4/u_1 &= f_4(M_1, M_{SL}), \\
 a_4/a_1 &= f_2(M_1, M_{SL})^{\frac{1}{2}} f_1(M_1, M_{SL})^{-\frac{1}{2}}, & M_4 &= f_5(M_1, M_{SL}),
 \end{aligned} \tag{4.1}$$

where $M_{SL} = s_L/a_1$ is called the shock Mach number of WL_1 .

We now turn to the overall relations of the solution. According to (2.6), the relations of the stationary discontinuity at the origin are

$$\frac{p_5}{p_4} = \psi(M_4) = \psi(f_5(M_1, M_{SL})), \quad (4.2a)$$

$$\frac{u_5}{u_4} = \phi(M_4) = \phi(f_5(M_1, M_{SL})). \quad (4.2b)$$

It is obtained from the shock relation of WR_3 that

$$u_5 - u_8 = \sqrt{\frac{\beta p_8}{\rho_8} \frac{p_5/p_8 - 1}{\sqrt{1 + \tau p_5/p_8}}}$$

where $\beta = 2/(\gamma - 1)$, $\tau = (\gamma + 1)/(\gamma - 1)$.

Substituting (4.1) and (4.2) into the above equation, we get

$$M_1(f_4(M_1, M_{SL})\phi(M_4) - 1) - \sqrt{\frac{\beta}{\gamma} \frac{f_2(M_1, M_{SL})\psi(M_4) - 1}{\sqrt{1 + \tau f_2(M_1, M_{SL})\psi(M_4)}}} = 0. \quad (4.3)$$

The equation (4.1) forms a system of equations for M_{SL} and M_4 as follows.

$$\begin{cases} M_1(f_4(M_1, M_{SL})\phi(M_4) - 1) - \sqrt{\frac{\beta}{\gamma} \frac{f_2(M_1, M_{SL})\psi(M_4) - 1}{\sqrt{1 + \tau f_2(M_1, M_{SL})\psi(M_4)}}} = 0 \\ M_4 = \frac{((\gamma - 1)M_1 + 2M_{SL})(M_1 - M_{SL}) + 2}{\sqrt{2\gamma(\gamma - 1)(M_1 - M_{SL})^4 + (6\gamma - \gamma^2 - 1)(M_1 - M_{SL})^2 - 2(\gamma - 1)}} \end{cases} \quad (4.4)$$

Another preliminary theorem is to conclude that M_{SL} can be expressed as a function of M_1 and M_4 in the solution of Type 1 or Type 2. From the Lax entropy condition of the shock (see [19]), we have

$$M_1 - M_{SL} = \frac{u_1 - s_L}{a_1} \geq 1. \quad (4.5)$$

Lemma 4.1 *Given any M_1 and M_4 , the M_{SL} satisfying $M_4 = f_5(M_1, M_{SL})$ and $M_1 - M_{SL} \geq 1$ exists and is unique.*

Proof 4.1 *The formula $M_4 = f_5(M_1, M_{SL})$ has another form.*

$$\begin{aligned} & M_4 \sqrt{(\gamma - 1)(M_1 - M_{SL})^2 + 2} \sqrt{2\gamma(M_1 - M_{SL})^2 - \gamma + 1} \\ &= -2(M_1 - M_{SL})^2 + (\gamma + 1)M_1(M_1 - M_{SL}) + 2. \end{aligned}$$

Dividing both sides of the above equation by $M_1 - M_{SL}$, we have

$$\begin{aligned} & M_4 \sqrt{(\gamma - 1)(M_1 - M_{SL})^2 + 2} \sqrt{2\gamma - \frac{\gamma + 1}{(M_1 - M_{SL})^2}} \\ &= -2(M_1 - M_{SL}) + (\gamma + 1)M_1(M_1 - M_{SL}) + \frac{2}{(M_1 - M_{SL})^2}. \end{aligned}$$

We define

$$\begin{aligned} \sigma_1(x) &\stackrel{def}{=} M_4 \sqrt{(\gamma - 1)x^2 + 2} \sqrt{2\gamma - \frac{\gamma + 1}{x^2}}, \\ \sigma_2(x) &\stackrel{def}{=} 2x - (\gamma + 1)M_1 - \frac{2}{x}, \\ \sigma(x) &\stackrel{def}{=} \sigma_1(x) + \sigma_2(x). \end{aligned}$$

The domains of $\sigma_1(x)$, $\sigma_2(x)$ and $\sigma(x)$ are $\{x|x \geq 1\}$. Both $\sigma_1(x)$ and $\sigma_2(x)$ are monotone increasing functions, hence $\sigma(x)$ is a monotone increasing function. It is clear that

$$\sigma(1) = (\gamma + 1)(M_4 - M_1) \leq 0,$$

$$\lim_{x \rightarrow \infty} \sigma(x) = \lim_{x \rightarrow \infty} \sigma_1(x) + \lim_{x \rightarrow \infty} \sigma_2(x) = \infty.$$

Consequently, the root of $\sigma(x)$ exists and is unique. $M_1 - M_{SL}$ is the root of $\sigma(x)$, and this completes the proof.

For the solutions of Type 1 and Type 2, it clear that

$$M_4 = \frac{((\gamma - 1)M_1 + 2M_{SL})(M_1 - M_{SL}) + 2}{\sqrt{2\gamma(\gamma - 1)(M_1 - M_{SL})^4 + (6\gamma - \gamma^2 - 1)(M_1 - M_{SL})^2 - 2(\gamma - 1)}}.$$

Treating $M_1 - M_{SL}$ as the variable, we have

$$A(M_1 - M_{SL})^4 + B(M_1 - M_{SL})^3 + C(M_1 - M_{SL})^2 + D(M_1 - M_{SL}) + E = 0, \quad (4.6)$$

where

$$\begin{aligned} A &= 4 - 2\gamma(\gamma - 1)M_4^2, \\ B &= -4(\gamma + 1)M_1, \\ C &= (\gamma + 1)^2M_1^2 - 8 - (6\gamma - \gamma^2 - 1)M_4^2, \\ D &= 4(\gamma + 1)M_1, \\ E &= 4 + 2(\gamma - 1)M_4^2. \end{aligned}$$

$M_1 - M_{SL}$ is the root of a fourth-order polynomial function (4.6). According to Lemma 4.1, We have proved the following theorem.

Theorem 4.1 *For the solutions of Type 1 and Type 2, M_{SL} can be expressed as $M_{SL} = f_6(M_1, M_4)$, which satisfies $M_4 = f_5(M_1, M_{SL})$ and $M_1 - M_{SL} \geq 1$.*

Now we turn to the uniqueness of the solution. The proof consists of two parts, one involves the states at the intermediate regions (Lemma 4.2), and the other is a division of these three structures (Lemma 4.3). Both of these are related to the Mach number M_1 of the initial flow.

We describe the strength of each nonlinear wave in terms of the ratio of pressures on both sides of this wave.

Lemma 4.2 *For these three types of solutions, the strength of each nonlinear wave is determined by the Mach number M_1 , independent of other variables.*

A proof of this lemma will be given in Appendix 6.

We define

$$X(M_1, M_4) \stackrel{def}{=} M_1(f_4(M_1, M_{SL})\phi(M_4) - 1) - \sqrt{\frac{\beta}{\gamma} \frac{f_2(M_1, M_{SL})\psi(M_4) - 1}{\sqrt{1 + \tau f_2(M_1, M_{SL})\psi(M_4)}}}, \quad (4.7)$$

and

$$Y(M_1) \stackrel{def}{=} X(M_1, M_*), \quad (4.8)$$

where $M_{SL} = f_6(M_1, M_4)$.

If $k(\gamma^2 - 1) \geq 1$, then M_{**} does not exist. Therefore the upstream flow of the heating point must be a subsonic flow. At this time, there are only two possible structures: Type 1 and Type 2. In this case, the downstream fluid must be subsonic. When $k(\gamma^2 - 1) < 1$, all three structures are possible. We associate the three structures with M_1 by the following lemma.

Lemma 4.3 *Under the double CRPs frame, the structures of the exact solution can only be Type 1 or Type 2 for $k(\gamma^2 - 1) \geq 1$, and all three structures are possible for $k(\gamma^2 - 1) < 1$. This type of solution satisfies the following conditions.*

- (i) *For the solution of Type 1, $Y(M_1) \geq 0$ holds;*
- (ii) *For the solution of Type 2, $Y(M_1) \leq 0$ and $M_1 \geq M_*$ hold, and $M_1 \leq M_{**}$ holds at the case of $k(\gamma^2 - 1) < 1$;*
- (iii) *For the solution of Type 3, $M_1 \geq M_{**}$ holds.*

A proof of this lemma will be given in Appendix 6.

It can be seen from Lemma 4.3 that the structure of M_1 equaling to the root of $Y(M_1)$ is the demarcation structure of Type 1 and Type 2, which is

$$S(U_1, U_4) \oplus H(U_4, U_5) \oplus C(U_5, U_7) \oplus S(U_7, U_8) \quad \text{with} \quad M_4 = M_*.$$

And the structure of M_1 equaling to M_{**} is the demarcation structure of Type 2 and Type 3, which is

$$S(U_1, U_4) \oplus H(U_4, U_5) \oplus R(U_5, U_6) \oplus C(U_6, U_7) \oplus S(U_7, U_8) \quad \text{with} \quad s_L = 0, \quad (4.9)$$

or

$$H(U_1, U_5) \oplus R(U_5, U_6) \oplus C(U_6, U_7) \oplus S(U_7, U_8) \quad \text{with} \quad M_5 = 1. \quad (4.10)$$

Remark 4.1 *The structure of (4.9) is a limit structure of Type 2. WL_1 is a normal shock and $M_4 = M_*$ hold for this structure, and it is clear that $M_1 = M_{**}$. For the structure of (4.10), $M_5 = 1$ implies $M_1 = M_{**}$. Therefore the structure of (4.9) equals to the structure of (4.10).*

According to Lemma 4.2 and Lemma 4.3, we can establish the following theorem.

Theorem 4.2 *Under the double CRPs frame, we have*

- (i) *if $k(\gamma^2 - 1) \geq 1$, the solution of Riemann problem (1.1) and (1.2) is unique;*
- (ii) *if $k(\gamma^2 - 1) < 1$, the solution of Riemann problem (1.1) and (1.2) is unique under the assumption that the root of $Y(M_1)$ is not greater than M_{**} .*

If the root of $Y(M_1)$ is greater than M_{**} , the uniqueness of the solution has not been proved. To compare the size of the root of $Y(M_1)$ and M_{**} , we define

$$R(\gamma, k) = \{M | Y(M) = 0\}, \quad T(\gamma, k) = M_{**} - R(\gamma, k).$$

Figure 4 shows the contour of the function T . The curved boundary on the upper right is the curve of $k(\gamma^2 - 1) = 1$. From Figure 4 it can be found $T(\gamma, k) > 0$, therefore the root of $Y(M_1)$ is smaller than M_{**} and the assumption in the second part of Theorem 4.2 is true. Thus we give the following conjecture.

Conjecture 4.1 *Under the double CRPs frame, the solution of Riemann problem (1.1) and (1.2) is unique for any given γ and κ , and the structure of the self-similar solution is determined by M_1 , as shown below.*

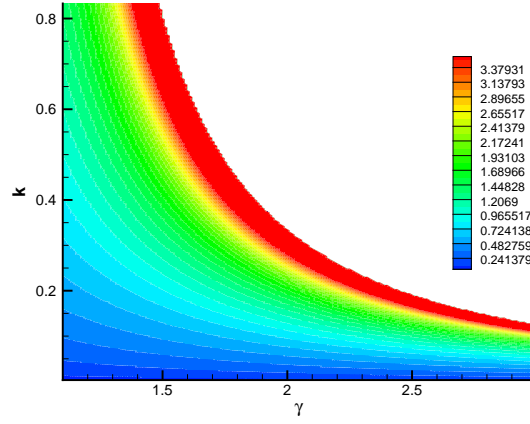


Figure 7: The contour of function $T(\gamma, k)$

- (i) If $Y(M_1) \geq 0$, the structure of the solution is Type 1.
- (ii) If $Y(M_1) \geq 0$ and $M_1 \leq M_{**}(k(\gamma^2 - 1) < 1)$, the structure of the solution is Type 2.
- (iii) If $k(\gamma^2 - 1) < 1$ and $M_1 \geq M_{**}$, the structure of the solution is Type 3.

5 Algorithm of Solution and Verification

Lemma 4.3 makes it legitimate to apply M_1 to determine the structure of the exact solution. Once the structure is determined, the solution becomes easy. A algorithm for the solution is given in Algorithm 1.

In the algorithm of Type 2, we use the bisection method to solve

$$M_* = \frac{((\gamma - 1)M_1 + 2M_{SL})(M_1 - M_{SL}) + 2}{\sqrt{2\gamma(\gamma - 1)(M_1 - M_{SL})^4 + (6\gamma - \gamma^2 - 1)(M_1 - M_{SL})^2 - 2(\gamma - 1)}}. \quad (5.1)$$

In the algorithm of Type 1, we do not iteratively solve 4.4, but use the pressure equations

$$u_1 + f_R(p_4\psi(M_4(p_4))) - \phi(M_4(p_4))(u_1 - f_L(p_4)) = 0,$$

where

$$M_4(p_4) = [u_1 - f_L(p_1)] \left[\frac{\rho_1}{\gamma} \frac{\gamma + 1 + (\gamma - 1)p_1/p_4}{(\gamma - 1)p_4 + (\gamma + 1)p_1} \right]^{\frac{1}{2}},$$

Algorithm 1 The Construction Algorithm of the Exact Solution

Input: the initial condition: $\rho_1, u_1, p_1, M_1, a_1$;

Output: the intermediate states: $W_4 = (\rho_4, u_4, p_4), W_5 = (\rho_5, u_5, p_5), W_6 = (\rho_6, u_6, p_6), W_7 = (\rho_7, u_7, p_7)$;

compute M_* and M_{**} ;

compute $Y(M_1)$;

if $M_1 \geq M_{**}$ **then**

$W_4 \leftarrow W_1$;

compute W_5 by (2.2);

else if $Y(M_1) \geq 0$ **then**

set the initial values of the bisection method: x_1, x_2 ;

$x_0 \leftarrow (x_1 + x_2)/2$;

set the value of termination condition: *error*;

while $|x_1 - x_2| > error$ **do**

$f_1 \leftarrow ((\gamma-1)M_1 + 2x_1)(M_1 - x_1) + 2 - M_*(2\gamma(\gamma-1)(M_1 - x_1)^4 + (6\gamma - \gamma^2 - 1)(M_1 - x_1)^2 - 2(\gamma-1))^{\frac{1}{2}}$;

$f_2 \leftarrow ((\gamma-1)M_1 + 2x_2)(M_1 - x_1) + 2 - M_*(2\gamma(\gamma-1)(M_1 - x_2)^4 + (6\gamma - \gamma^2 - 1)(M_1 - x_2)^2 - 2(\gamma-1))^{\frac{1}{2}}$;

if $f_1 \times f_2 < 0$ **then**

$x_0 \leftarrow x_1$;

else

$x_1 \leftarrow x_0$;

end if

$x_0 \leftarrow (x_1 + x_2)/2$;

end while

$\rho_4 \leftarrow \rho_1 f_1(M_1, x_0), u_4 \leftarrow u_1 f_4(M_1, x_0), p_4 \leftarrow p_1 f_2(M_1, x_0), M_4 \leftarrow M_*$;

compute W_5 by (2.1);

$p_5 \leftarrow p_4 \psi(M_*), u_5 \leftarrow u_4 \phi(M_*), \rho_5 \leftarrow (\rho_4 u_4)/u_5$;

else

// f_L and f_R are given by (5.2).

set the initial values of the bisection method: y_1, y_2 ;

$y_0 \leftarrow (y_1 + y_2)/2$;

set the value of termination condition: *error*;

while $|y_1 - y_2| > error$ **do**

$m_1 \leftarrow (u_1 - f_L(y_1)) \left[\frac{\rho_1}{\gamma} \frac{\gamma+1+(\gamma-1)p_1/y_1}{(\gamma-1)y_1+(\gamma+1)p_1} \right]^{\frac{1}{2}}, m_2 \leftarrow (u_1 - f_L(y_2)) \left[\frac{\rho_1}{\gamma} \frac{\gamma+1+(\gamma-1)p_1/y_2}{(\gamma-1)y_2+(\gamma+1)p_1} \right]^{\frac{1}{2}}$;

$g_1 \leftarrow u_1 + f_R(y_1 \psi(m_1)) - \phi(m_1)(u_1 - f_L(y_1)), g_2 \leftarrow u_1 + f_R(y_2 \psi(m_2)) - \phi(m_1)(u_1 - f_L(y_2))$;

if $g_1 \times g_2 < 0$ **then**

$y_0 \leftarrow y_1$;

else

$y_1 \leftarrow y_0$;

end if

$y_0 \leftarrow (y_1 + y_2)/2$;

end while

$\rho_4 \leftarrow \rho_1 \frac{(\gamma-1)p_1+(\gamma+1)y_0}{(\gamma-1)y_0+(\gamma+1)p_1}, u_4 \leftarrow u_1 - f_L(y_0), p_4 \leftarrow y_0$;

$M_1 \leftarrow (u_1 - f_L(y_0)) \left[\frac{\rho_1}{\gamma} \frac{\gamma+1+(\gamma-1)p_1/y_0}{(\gamma-1)y_0+(\gamma+1)p_1} \right]^{\frac{1}{2}}$;

compute W_5 by (2.1);

end if

compute W_6 and W_7 by a Riemann solver $CRP(W_5, W_8)$.

$$\begin{aligned}
 f_L(p) &= \begin{cases} (p - p_1) \left[\frac{A_L}{p+B_L} \right]^{\frac{1}{2}}, & \text{if } p > p_1 \\ \frac{2a_1}{\gamma-1} \left[\left(\frac{p}{p_1} \right)^{\frac{\gamma-1}{2\gamma}} - 1 \right], & \text{if } p \leq p_1 \end{cases}, \\
 f_R(p) &= \begin{cases} (p - p_1) \left[\frac{A_R}{p+B_R} \right]^{\frac{1}{2}}, & \text{if } p > p_1 \\ \frac{2a_1}{\gamma-1} \left[\left(\frac{p}{p_1} \right)^{\frac{\gamma-1}{2\gamma}} - 1 \right], & \text{if } p \leq p_1 \end{cases}.
 \end{aligned} \tag{5.2}$$

A_L, A_R, B_L, B_R are given by

$$A_L = \frac{2}{(\gamma + 1)\rho_1}, B_L = \frac{\gamma - 1}{\gamma + 1}p_1, A_R = \frac{2}{(\gamma + 1)\rho_1}, B_R = \frac{\gamma - 1}{\gamma + 1}p_1.$$

Experiments show that this iterative method is less sensitive to the initial value of the iteration. Lemma 4.1 guarantees that the solution of the iterative equation in the algorithm is unique. A classical Riemann solver $CRP(W_5, W_8)$ of the Euler equations is needed in the algorithm. The wave pattern is identical for this CRP, which consists a rarefaction wave corresponding to the $u - a$ characteristic field and a shock wave corresponding to the $u + a$ characteristic field.

We verify the existence of these three structures through numerical tests, and compare the states of the constructed self-similar solution with the numerical solution at intermediate regions. The following five tests are all for the ideal gas with $\gamma = 1.4$, and their exact solutions cover three proposed structures. The initial conditions and heating parameters of the five tests are shown in Table 1. The comparison between the numerical solutions and the

Table 1: Initial conditions and parameter setting in experiments

	initial conditions			heating parameter	solution structure
	ρ	u	p		
Test1	1.0	0.8	1.0	0.2	Type 1
Test2	1.0	1.2	1.0	0.2	Type 1
Test3	1.0	1.8	1.0	0.2	Type 2
Test4	1.0	2.8	1.0	0.2	Type 3
Test5	1.0	2.8	1.0	2.0	Type 2

exact solutions are shown in Figure??. In the first four tests, the heating parameter is $k = 0.2$, and $k(\gamma^2 - 1) < 1$ holds. M_* and M_{**} are 0.6136 and 1.8130, respectively. The root of $Y(M_1)$ is 1.0620, which is less than M_{**} , hence the solution is unique. In the last test, the value of k

is 2.0. $k(\gamma^2 - 1) > 1$ holds at this time. According to Theorem 4.2, the exact solutions of these

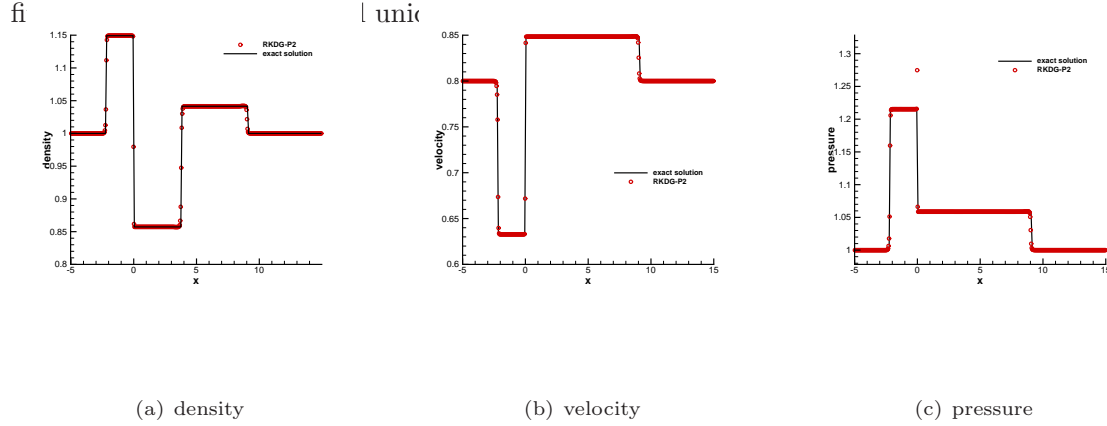


Figure 8: The numerical solution obtained by the RKDG and comparison to the constructed self-similar solution for Test1 at $t = 4.5s$.

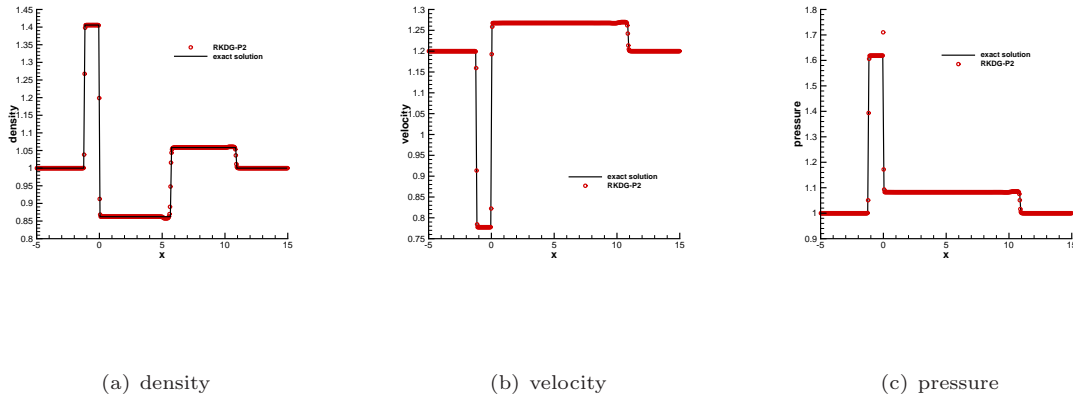
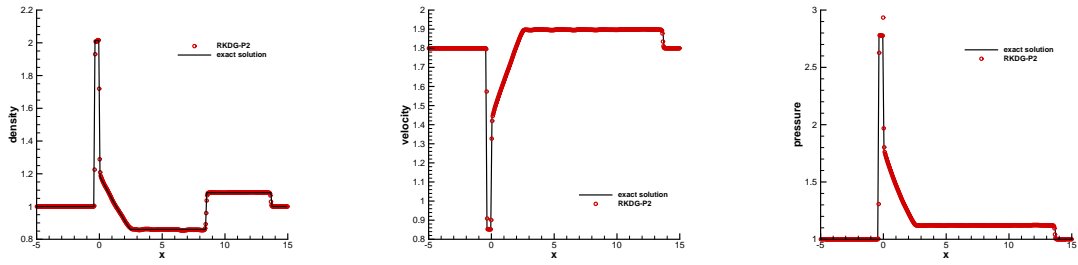


Figure 9: The numerical solution obtained by the RKDG and comparison to the constructed self-similar solution for Test2 at $t = 4.5s$.

We apply the Runge-Kutta discontinuous Galerkin method (RKDG) for numerical simulation (see [26]). In the spatial direction, the solution is discretized by piece-wise second-order ($P2$) polynomials. A total variation diminishing (TVD) limiter is employed to avoid numerical oscillations. In the time direction, we use the third-order Runge-Kutta method. The source is processed through splitting. Note that the source term should be processed at each time step of Runge-Kutta method.

It can be observed from figures that the constructed exact solution and numerical solution fit well in each intermediate regions. While inside several cells near origin, the solutions of

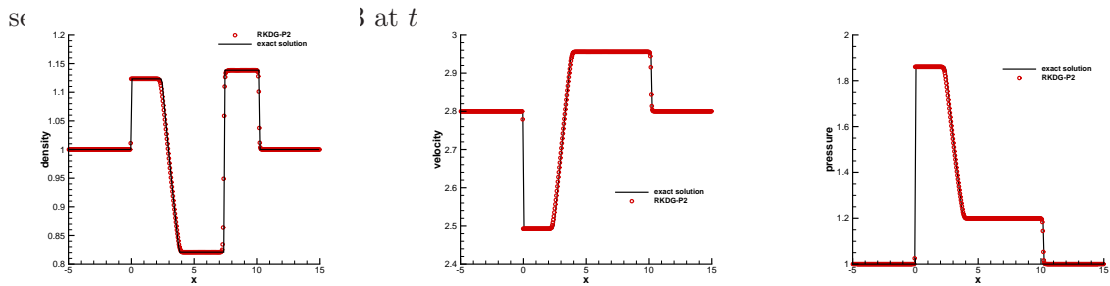


(a) density

(b) velocity

(c) pressure

Figure 10: The numerical solution obtained by the RKDG and comparison to the constructed

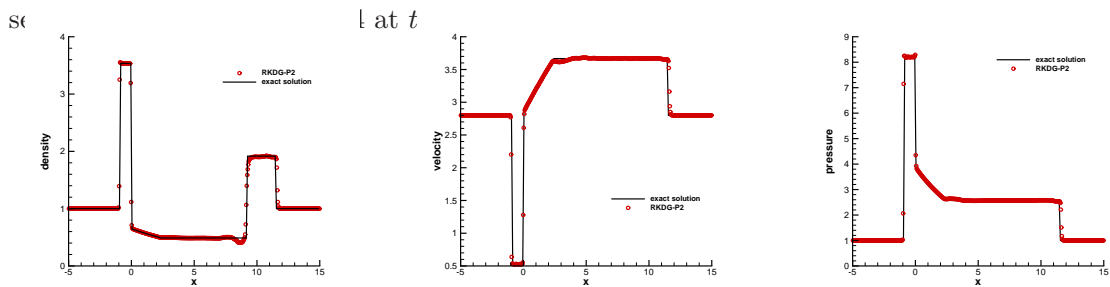


(a) density

(b) velocity

(c) pressure

Figure 11: The numerical solution obtained by the RKDG and comparison to the constructed



(a) density

(b) velocity

(c) pressure

Figure 12: The numerical solution obtained by the RKDG and comparison to the constructed self-similar solution for Test5 at $t = 2.5s$.

pressure are some different between the exact solution and the numerical solution. The reason is that directly splitting the source term has no "well-balanced" property.

6 Conclusions

This paper focused on the Riemann problem of the Euler equations with a Dirac delta-source in the energy conservation equation. The double CRPs frame was proposed to construct the self-similar solutions. We proved that there are three types of the solution and studied the uniqueness of the solutions under this frame. The present frame is completely different from the existing method of dealing with the Riemann problem with discontinuous source. Based on the solution of CRP, the strategy of the present frame is the elimination of unconservation waves on the general structure (Figure 3). This frame can be applied to the Riemann problem of other hyperbolic systems with Dirac delta-function sources or other sources. Compared with some existing methods, it is more simple and can naturally cover all possible structures. We verified the double CRPs frame by comparing the constructed self-similar solution with the numerical solution obtained by RKDG. Besides, the constructed solutions can be used to evaluate the existing numerical methods for source terms, such as [11–13].

The uniqueness of the self-similar solutions under the double CRPs frame for arbitrary initial conditions is an open question, which is the goal of our future work. In addition, future work should focus on the heating addition of unsteady flow, in which the transition of the three structures proposed in this paper may occur.

Appendix

Proof of Lemma 4.2

Proof 6.1 For the solution of Type 1, (4.1) and (4.2) imply

$$\begin{aligned} p_4/p_1 &= f_2(M_1, M_{SL}), \\ p_8/p_7 &= p_1/p_4 \times p_4/p_5 = [f_2(M_1, M_{SL})\psi(f_5(M_1, M_{SL}))]^{-1}, \end{aligned}$$

where M_{SL} is obtained from equation (4.4) and is determined by M_1 .

For Structure 2, we have

$$p_4/p_1 = f_2(M_1, M_{SL}),$$

where M_{SL} is obtained from equation (5.1) and is determined by M_1 .

From the elementary wave equation in [23], we have

$$u_6 = u_5 - \frac{2a_5}{\gamma - 1} \left[\left(\frac{p_6}{p_5} \right)^{\frac{\gamma-1}{2\gamma}} - 1 \right],$$

$$u_7 = u_8 + \sqrt{2}(p_7 - p_8) [(\gamma + 1)p_7\rho_8 + (\gamma - 1)p_8\rho_8]^{-\frac{1}{2}}.$$

According to $u_6 = u_7$, $p_6 = p_7$ and $U_1 = U_8$, it follows that

$$u_5 - \frac{2a_5}{\gamma - 1} \left[\left(\frac{p_6}{p_5} \right)^{\frac{\gamma-1}{2\gamma}} - 1 \right] = u_1 + \sqrt{2}(p_6 - p_1) [(\gamma + 1)p_6\rho_1 + (\gamma - 1)p_1\rho_1]^{-\frac{1}{2}}.$$

Divide both sides of the above equation by a_1 , then

$$\frac{u_5}{u_1} M_1 - \frac{2}{\gamma - 1} \frac{M_1}{M_5} \frac{u_5}{u_1} \left[\left(\frac{p_6}{p_5} \right)^{\frac{\gamma-1}{2\gamma}} - 1 \right] = M_1 + \frac{\sqrt{2}}{a_1} (p_6 - p_1) [(\gamma + 1)p_6\rho_1 + (\gamma - 1)p_1\rho_1]^{-\frac{1}{2}}.$$

Apply the equation of state to the above equation, we have

$$\frac{u_5}{u_1} M_1 - \frac{2}{\gamma - 1} \frac{M_1}{M_5} \frac{u_5}{u_1} \left[\left(\frac{p_6}{p_5} \right)^{\frac{\gamma-1}{2\gamma}} - 1 \right] = M_1 + \sqrt{\frac{2}{\gamma}} \left(\frac{p_6}{p_1} - 1 \right) \left[(\gamma + 1) \frac{p_6}{p_1} + (\gamma - 1) \right]^{-\frac{1}{2}}.$$

Therefore

$$\left(A \left(\frac{p_6}{p_5} \right)^{\frac{\gamma-1}{2\gamma}} + B \right) \sqrt{C \frac{p_6}{p_5} + \gamma - 1} - \sqrt{\frac{2}{\gamma}} \left(\frac{C}{\gamma + 1} \frac{p_6}{p_5} - 1 \right) = 0,$$

where $A = -\frac{2}{\gamma-1} M_1 \phi(M_*) f_4(M_1, M_{SL})$, $B = \frac{\gamma+1}{\gamma-1} M_1 \phi(M_*) f_4(M_1, M_{SL})$, $C = (\gamma + 1) \psi(M_*) f_2(M_1, M_{SL})$ and M_{SL} is obtained from (5.1). Thus the strength of WR_1 in the solution of Type 2 is determined by M_1 .

For WR_3 , we have

$$\frac{p_8}{p_7} = \left[f_2(M_1, M_{SL}) \psi(M_*) \frac{p_6}{p_5} \right]^{-1}.$$

Therefore the strength of each nonlinear wave in the solution of Type 2 is determined by M_1 .

The analyse of Type 3 is similar, as follows.

$$\left(A' \left(\frac{p_6}{p_5} \right)^{\frac{\gamma-1}{2\gamma}} + B' \right) \sqrt{C' \frac{p_6}{p_5} + \gamma - 1} - \sqrt{\frac{2}{\gamma}} \left(\frac{C'}{\gamma + 1} \frac{p_6}{p_5} - 1 \right) = 0,$$

$$\frac{p_8}{p_7} = \left[\frac{p_5 p_6}{p_1 p_5} \right]^{-1},$$

where $A' = -\frac{2}{\gamma-1} \frac{M_1 u_5}{M_5 u_1}$, $B' = \frac{u_5}{u_1} M_1 + \frac{2}{\gamma-1} \frac{M_1 u_5}{M_5 u_1}$, $C' = (\gamma+1) \frac{p_5}{p_1} \cdot \frac{u_5}{u_1}$, $\frac{p_5}{p_1}$ and M_5 in the above equation are obtained from Lemma 3.1 and they are all determined by M_1 .

Proof of Lemma 4.3

Proof 6.2 From (4.3), we have

$$X(M_1, M_4) = 0.$$

Some tedious manipulation yields

$$\frac{\partial f_5}{\partial M_{SL}} > 0,$$

and

$$\frac{\partial f_6}{\partial M_{SL}} = \left(\frac{\partial f_5}{\partial M_{SL}} \right)^{-1} > 0.$$

Then

$$\frac{\partial X}{\partial M_4} = M_1 \frac{\partial}{\partial M_4} (f_4(M_1, M_{SL}) \phi(M_4)) - \sqrt{\frac{\beta}{\gamma}} \frac{\partial}{\partial M_4} \left(\frac{f_2(M_1, M_{SL}) \psi(M_4) - 1}{\sqrt{1 + \tau f_2(M_1, M_{SL}) \psi(M_4)}} \right). \quad (6.1)$$

For the first part on the right of (6.1), we have

$$\begin{aligned} \frac{\partial}{\partial M_4} (f_4(M_1, M_{SL}) \phi(M_4)) &= \frac{\partial f_4(M_1, M_4)}{\partial M_4} \phi(M_4) + \frac{d\phi(M_4)}{dM_4} f_4(M_1, M_{SL}), \\ \frac{\partial f_4(M_1, M_4)}{\partial M_4} &= \frac{\partial f_4(M_1, M_4)}{\partial M_{SL}} \frac{\partial M_{SL}}{\partial M_4} = \frac{2(1 + (M_1 - M_{SL})^{-2})}{(\gamma+1)M_1} \frac{\partial f_6}{\partial M_4} > 0, \\ \phi'(M_4) &> 0. \end{aligned}$$

Thus

$$\frac{\partial}{\partial M_4} (f_4(M_1, M_{SL}) \phi(M_4)) > 0.$$

For the second part on the right of (6.1), we have

$$\begin{aligned} \frac{\partial}{\partial M_4} \left(\frac{f_2(M_1, M_{SL}) \psi(M_4) - 1}{\sqrt{1 + \tau f_2(M_1, M_{SL}) \psi(M_4)}} \right) &= \frac{\tau(f_2(M_1, M_{SL}) \psi(M_4) + 1) + 2}{2(f_2(M_1, M_{SL}) \psi(M_4))^{3/2}} \frac{\partial}{\partial M_4} (f_2(M_1, M_{SL}) \psi(M_4)), \\ \frac{\partial}{\partial M_4} (f_2(M_1, M_{SL}) \psi(M_4)) &= - \left(\frac{\partial f_2}{\partial M_1} - \frac{\partial f_2}{\partial M_{SL}} \right) \psi(M_4) + \frac{d\psi(M_4)}{dM_{SL}} f_2(M_1, M_{SL}), \\ \frac{\partial f_2}{\partial M_1} - \frac{\partial f_2}{\partial M_{SL}} &> 0, \\ \psi'(M_4) &< 0. \end{aligned}$$

Thus

$$\frac{\partial}{\partial M_4}(f_2(M_1, M_{SL})\psi(M_4)) < 0,$$

and

$$\frac{\partial}{\partial M_4} \left(\frac{f_2(M_1, M_{SL})g_2(M_1, M_{SL}) - 1}{\sqrt{1 + \tau f_2(M_1, M_{SL})g_2(M_1, M_{SL})}} \right) < 0.$$

Note that we have actually proved that

$$\frac{\partial X}{\partial M_4} > 0.$$

According to Lemma 2.1, it follows that $M_4 < M_*$. Consequently

$$Y(M_1) = X(M_1, M_*) \geq X(M_1, M_4) = 0.$$

Proof 6.3 The solution right to the t -axis of Type 2 is the solution of CRP(U_5, U_8), whose wave pattern is $R(U_5, U_6) \oplus C(U_6, U_7) \oplus S(U_7, U_8)$, it follows that (see [16])

$$u_5 - u_8 \leq \sqrt{\frac{\beta p_8}{\rho_8} \frac{p_5/p_8 - 1}{\sqrt{1 + \tau p_5/p_8}}}.$$

Represent the above equation by the Mach numbers, as follows.

$$M_1(f_4(M_1, M_{SL})\phi(M_*) - 1) - \sqrt{\frac{\beta}{\gamma} \frac{f_2(M_1, M_{SL})\psi(M_*) - 1}{\sqrt{1 + \tau f_2(M_1, M_{SL})\psi(M_*)}}} \leq 0.$$

Thus

$$Y(M_1) \leq 0.$$

We denote

$$M'_{SL} = \frac{s_L}{a_4},$$

where s_L is the speed of WL_1 and a_4 is the speed of sound in region 4. Similar to (4.1), it holds that

$$M_1 = \frac{((\gamma - 1)M_4 + 2M'_{SL})(M_4 - M'_{SL}) + 2}{\sqrt{2\gamma(\gamma - 1)(M_4 - M'_{SL})^4 + (6\gamma - \gamma^2 - 1)(M_4 - M'_{SL})^2 - 2(\gamma - 1)}}.$$

Define

$$g(M_4, M'_{SL}) = \frac{((\gamma - 1)M_4 + 2M'_{SL})(M_4 - M'_{SL}) + 2}{\sqrt{2\gamma(M_4 - M'_{SL})^2 - \gamma + 1}\sqrt{(\gamma - 1)(M_4 - M'_{SL})^2 + 2}}.$$

The domain of g satisfies

$$M_4 \leq M_*, \quad M'_{SL} \leq 0.$$

A routine computation gives rise to

$$\frac{\partial g}{\partial M'_{SL}} > 0.$$

Then

$$g(M_4, M'_{SL}) \leq g(M_4, 0) = \sqrt{\frac{(\gamma - 1)M_4^2 + 2}{2\gamma M_4^2 - \gamma + 1}},$$

and

$$M_1 = g(M_*, M'_{SL}) \leq g(M_*, 0) = \sqrt{\frac{(\gamma - 1)M_*^2 + 2}{2\gamma M_*^2 - \gamma + 1}}.$$

According to Lemma 2.2, it follows that

$$M_1 \leq M_{**}.$$

The proof of (iii) is obvious.

Acknowledgments

This work was supported by the NSFC-NSAF joint fund [No. U1730118]; and the Science Challenge Project [No. JCKY2016212A502].

References

- [1] Rémi Abgrall and Smadar Karni. A comment on the computation of non-conservative products. *Journal of Computational Physics*, 229(8):2759–2763, 2010.
- [2] Francisco Alcrudo and Fayssal Benkhaldoun. Exact solutions to the riemann problem of the shallow water equations with a bottom step. *Computers & Fluids*, 30(6):643 – 671, 2001.
- [3] Matania Benartzi and Joseph Falcovitz. A second-order godunov-type scheme for compressible fluid dynamics. *Journal of Computational Physics*, 55(1):1–32, 1984.
- [4] Matania Benartzi, Jiequan Li, and Gerald Warnecke. A direct eulerian grp scheme for compressible fluid flows. *Journal of Computational Physics*, 218(1):19–43, 2006.
- [5] R Bernetti, V A Titarev, and Eleuterio F Toro. Exact solution of the riemann problem for the shallow water equations with discontinuous bottom geometry. *Journal of Computational Physics*, 227(6):3212–3243, 2008.

-
- [6] Wan Cheng, Xisheng Luo, and Van Meh Rini Dongen. On condensation-induced waves. *Journal of Fluid Mechanics*, 651(1):145–164, 2010.
- [7] Can F Delale, G H Schnerr, and Jurgen Zierep. The mathematical theory of thermal choking in nozzle flows. *Zeitschrift für Angewandte Mathematik und Physik*, 44(6):943–976, 1993.
- [8] Can F. Delale, Günter H. Schnerr, and Marinus E. H. Van Dongen. *Condensation Discontinuities and Condensation Induced Shock Waves*. 2007.
- [9] M. E. H. Van Dongen, X. Luo, G. Lamanna, and D. J. Van Kaathoven. On condensation induced shock waves. In *Proc. 10th Chinese Symposium on Shock Waves*, 2002.
- [10] Laurent Gosse. A well-balanced scheme using non-conservative products designed for hyperbolic systems of conservation laws with source terms. *Mathematical Models and Methods in Applied Sciences*, 11(02):339–365, 2001.
- [11] J M Greenberg, A Y Leroux, R Baraille, and A Noussair. Analysis and approximation of conservation laws with source terms. *SIAM Journal on Numerical Analysis*, 34(5):1980–2007, 1997.
- [12] Shi Jin and Xin Wen. Two interface-type numerical methods for computing hyperbolic systems with geometrical source terms having concentrations. *SIAM Journal on Scientific Computing*, 26(6):2079–2101, 2005.
- [13] Dietmar Kroner and Mai Duc Thanh. Numerical solutions to compressible flows in a nozzle with variable cross-section. *SIAM Journal on Numerical Analysis*, 43(2):796–824, 2005.
- [14] Philippe G Lefloch and Mai Duc Thanh. The riemann problem for fluid flows in a nozzle with discontinuous cross-section. *Communications in Mathematical Sciences*, 1(4):763–797, 2003.
- [15] Philippe G Lefloch and Mai Duc Thanh. The riemann problem for the shallow water equations with discontinuous topography. *Communications in Mathematical Sciences*, 5(4):865–885, 2007.
- [16] T G Liu, Boo Cheong Khoo, and C W Wang. The ghost fluid method for compressible gas-water simulation. *Journal of Computational Physics*, 204(1):193–221, 2005.

-
- [17] Xisheng Luo, B Bart Prast, Van Meh Rini Dongen, Hwm Harrie Hoeijmakers, and J Yang. On phase transition in compressible flows: modelling and validation. *Journal of Fluid Mechanics*, 548(1):403–430, 2006.
- [18] Carlos Pares and Ernesto Pimentel. The riemann problem for the shallow water equations with discontinuous topography: The wet–dry case. *Journal of Computational Physics*, 378:344–365, 2019.
- [19] D Peter. *Hyperbolic systems of conservation laws and the mathematical theory of shock waves* /. Society for Industrial and Applied Mathematics,, 1973.
- [20] Gunter Schnerr. Unsteadiness in condensing flow: Dynamics of internal flows with phase transition and application to turbomachinery. *Journal of Mechanical Engineering Science*, 219, 2005.
- [21] Mai Duc Thanh. The riemann problem for a nonisentropic fluid in a nozzle with discontinuous cross-sectional area. *Siam Journal on Applied Mathematics*, 69(6):1501–1519, 2009.
- [22] Mai Duc Thanh. Numerical treatment in resonant regime for shallow water equations with discontinuous topography. *Communications in Nonlinear Science and Numerical Simulation*, 18(2):417–433, 2013.
- [23] Eleuterio F. Toro. *Riemann solvers and numerical methods for fluid dynamics : a practical introduction*. Springer,.
- [24] Eleuterio F Toro and Arturo Hidalgo. Ader finite volume schemes for nonlinear reaction–diffusion equations. *Applied Numerical Mathematics*, 59(1):73–100, 2009.
- [25] Eleuterio F Toro and Gino I Montecinos. Implicit, semi-analytical solution of the generalized riemann problem for stiff hyperbolic balance laws. *Journal of Computational Physics*, 303:146–172, 2015.
- [26] Yang Yang and Chi-Wang Shu. Discontinuous galerkin method for hyperbolic equations involving δ -singularities: negative-order norm error estimates and applications. *Numerische Mathematik*, 124(4):753–781, 2013.